ChemElectroChem

Research Article
doi.org/10.1002/celc.202400415

Chemistry Europe
European Chemical Societies Publishing

www.chemelectrochem.org

Influence of Molecular Weight and End Groups on Ion Transport in Weakly and Strongly Coordinating Polymer Electrolytes

Rassmus Andersson[+],[a] Samuel Emilsson[+],[b] Guiomar Hernández,[a] Mats Johansson,[b] and Jonas Mindemark*[a]

In the development of polymer electrolytes, the understanding of the complex interplay of factors that affect ion transport is of importance. In this study, the strongly coordinating and flexible poly (ethylene oxide) (PEO) is compared to the weakly coordinating and stiff poly (trimethylene carbonate) (PTMC) as opposing model systems. The effect of molecular weight (M_n) and end group chemistry on the physical properties: glass transition temperature (T_g) and viscosity (η) and ion transport properties: transference number (T_+), ion coordination strength and ionic conductivities were investigated. The cation transference number (T_+) showed the opposite dependence on M_n for PEO and PTMC, decreasing at low M_n for PTMC and increasing for PEO. This was shown to be highly dependent on the ion coordination strength of the system regardless of whether the end group was OH or if the chains were end-capped. Although the coordination is mainly of the cations in the systems, the differences in T_+ were due to differences in anion rather than cation conductivity, with a similar Li^+ conductivity across the polymer series when accounting for the differences in segmental mobility.

Introduction

The exponentially increasing demand for lithium-ion batteries (LIBs) for energy storage rapidly pushes battery technology towards more energy-dense batteries. This has led to an emerging interest in lithium-metal batteries (LMBs), where the energy-dense lithium metal is used as the negative electrode. Utilization of lithium metal is, however, challenging due to dendritic plating of Li, resulting in metallic formations with a high surface area, which intensifies exothermic reactions with other cell components as well as the risk of short-circuiting the cell by penetrating the separator.[1] Solid polymer electrolytes (SPEs) have therefore gained interest due to their mechanical and thermal stability, improving the compatibility with lithium metal, as well as being less volatile than conventional liquid electrolytes. The relatively low cost and processability of SPEs also make them an attractive alternative for further development. Despite this, the relatively poor ionic conductivity compared to liquid electrolytes has resulted in the implementation of SPEs in LMBs having been significantly restrained, limiting their utilization in high-power-density applications.

Among SPE materials, polyethylene oxide (PEO) is by far the most extensively studied host material due to its ability to provide relatively high total ionic conductivity, low-cost production and non-toxicity. Furthermore, PEO is the only polymer host in SPEs implemented in battery cells and electric vehicles today. Not all ions are equal, however, and apart from the total ionic conductivity, the Li^+ transference number (T_+) is also an important parameter as a measure of the contribution of Li^+ to the total ionic conductivity. A high T_+ is beneficial for the system as it is less prone to generate concentration gradients and internal resistances in the cell, decreasing risks of cell failure and allowing higher discharge rates.[2] PEO-based electrolytes, however, are known for low Li transference numbers; *i.e.*, the main contributing species to the total conductivity are the anions which are redox-inactive in commonly used Li battery electrode materials. This has been explained by the strong coordination observed for Li^+ in PEO systems, where optimal coordination of the PEO chains around the Li-ions is created with multiple coordination sites, generating an energetically favorable environment.[3] In contrast, there are other host materials where the opposite is observed, *i.e.*, weak coordination between Li^+ and the polymer chains, leading to a high T_+, is poly (trimethylene carbonate) (PTMC).[3a,4] The opposite behaviors of PEO and PTMC, with the strongly coordinating and flexible PEO at one end of the spectrum and the weakly coordinating and stiff PTMC at the other, make comparisons between them particularly interesting.

Comparative studies on PEO and PTMC have so far only been made above 4000 g mol^{-1}, where the Li-ion transport

[a] R. Andersson,[+] G. Hernández, J. Mindemark
Department of Chemistry – Ångström Laboratory
Uppsala University
Box 538, SE-751 21 Uppsala, Sweden
E-mail: jonas.mindemark@kemi.uu.se

[b] S. Emilsson,[+] M. Johansson
Department of Fibre & Polymer Technology, Division of Coating Technology
KTH Royal Institute of Technology
SE-100 44 Stockholm, Sweden

[+] These authors contributed equally to this work and should be considered as co-first authors.

Supporting information for this article is available on the WWW under https://doi.org/10.1002/celc.202400415

properties remain relatively independent of molecular weight.[3a,5] How these properties evolve when transitioning from liquid-like systems at low molecular weight to solid systems at high molecular weights in different polymer hosts is therefore not fully understood yet. At the same time, oligomers are gaining growing interest as a compromise between liquid and solid.[6] A limitation with solid polymer electrolytes is their penetration into thick porous cathodes, which is necessary for achieving high energy densities.[7] For this reason, oligomers that maintain a level of flowability have the possibility of achieving better cathode infiltration. Meanwhile, the volatility of oligomers is still significantly lower than conventional liquid electrolytes, motivating the exploration of oligomers based on PEO, PTMC and poly (ε-caprolactone) (PCL) for battery implementation.[6,8]

What is known about the transition between low-molecular-weight oligomers and polymers has been primarily gleaned from studying PEO. In a pioneering study from Shi and Vincent,[9] the mobility of PEO and Li triflate complexes was studied for a range of molecular weights. The chain and cation mobilities were measured using diffusion NMR and correlated to viscosity measurements, showing that above a certain critical molecular weight, the cation mobility remains relatively constant. These findings were verified further through experimental efforts by Hayamizu et al.[10] and Teran et al.[5a] Diddens et al.[11] used MD simulations to look into the mechanisms behind the proposed shift in the ion transport mechanism of PEO chains with an increase in molecular weight M_n.

Timachova et al.[5c] studied the diffusion of LiTFSI in PEO in a large range of molecular weights and salt concentrations, showing their combined effects on the transference number. It was proposed that at low molecular weights and salt concentrations, the ion transport is coupled to the relaxation of the PEO chains that have an M_n dependence according to the Rouse model, while at high molecular weights and salt concentrations, the ion transport proceeds by solvation/desolvation events and is governed by segmental motion. Devaux et al.[5b] extensively studied the effect of molecular weight on the ionic conductivity and viscosity of PEO doped with LiTFSI. Below a critical molecular weight, the viscosity and ionic conductivity were significantly affected by the nature of the end group, where methyl end groups allowed for greater mobility than hydroxyl end groups due to an increase in free volume. The study also showed how the T_+ of the PEO-based electrolytes decreases with increasing molecular weight, eventually reaching a plateau value of around 0.15. Again, a shift in ion transport mechanism a function of M_n was proposed to explain the results. The effect of different end group on the interactions with Li^+, ionic conductivity and T_+ has also been investigated for other PEO-containing systems such as single-ion conducting PEO oligomers,[12] PEO blocks in PS-b-PEO copolymers,[13] and composite PEO electrolytes with grafted SiO_2 nanoparticles.[14]

While these investigations have provided a lot of details on ion transport in PEO, the comparison to other systems is lacking. PEO, with its unique chelating ability, is not representative of how all polymers behave, and it is therefore necessary to also look into how these effects change for different polymer systems. In this work, the effect of molecular weight is investigated for the physical properties of glass transition temperature (T_g) and viscosity (η) as well as ion transport properties: transference number, ion coordination strength and ionic conductivity. These properties are examined in the weakly ion-coordinating PTMC and compared to the well-studied and strongly ion-coordinating PEO, allowing for a detailed look at the effects of ion coordination on the connection between molecular weight and ion transport properties. Furthermore, the impact of the end groups on these properties is explored in PTMC and again contrasted to PEO, where samples with hydroxyl end groups and end-capped samples are analyzed. This work revises previous conclusions about the ion transport mechanism dependence on the M_n and what effect the segmental motion has for systems with low M_n. This is shown by emphasizing the close relationship between the coordination strength and the T_+ and its relevance for ion transport.

Experimental

Materials

PEO (M_n = 300, 600, 1000, 2000, 4000, 6000 g mol^{-1}) and end-capped PEO (M_n = 220, 500, 1000, 2000 g mol^{-1}) were purchased from Sigma-Aldrich and used as received. Note that the end-capped PEO with M_n = 220 g mol^{-1} is tetraethylene glycol dimethyl ether (TEGDME). PTMC (M_n = 400, 600, 850, 1050, 2000, 4250 g mol^{-1}) was synthesized by ring-opening polymerization of the monomer trimethylene carbonate (TMC, Richman Chemicals) in a stainless steel reactor over 72 h at 130 °C as described elsewhere.[3a] The end-capped PTMC (M_n = 220, 320, 530, 1040, 2060 g mol^{-1}) was synthesized in a two-step reaction in which the ring-opening polymerization of TMC was followed by end-capping of the hydroxyl end groups using ethyl chloroformate as described elsewhere.[8c] The sample with M_n = 220 was synthesized by end-capping 1,3-propanediol using ethyl chloroformate. The product was then purified through solvent extraction and dried under vacuum. The end-capped PTMC samples with M_n = 220 and 300 were also dried over molecular sieves. The structures of all polymers are shown in Figure 1. Lithium bis (trifluoromethanesulfonyl) imide (LiTFSI) was purchased from Solvionic and dried in a vacuum oven at 120 °C for 48 h. The solid polymer electrolytes were prepared by solution casting of dissolved polymers and LiTFSI in acetonitrile, which were added to polytetrafluoroethylene molds and the solvent evaporated under controlled conditions as described elsewhere.[3a] The

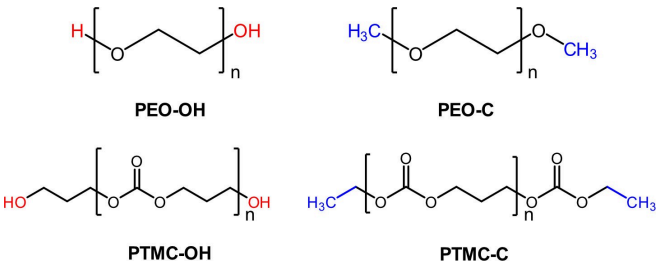

Figure 1. Chemical structures of poly (ethylene oxide) (PEO-OH), poly (ethylene oxide) dimethyl ether (PEO-C), poly (trimethylene carbonate) (PTMC-OH), and ethyl carbonate-capped poly (trimethylene carbonate) (PTMC-C).

salt concentration was kept at a ratio of $r = [LiTFSI]/[monomer] = 0.10$ for all SPEs.

Differential Scanning Calorimetry (DSC)

A Mettler Toledo DSC 3+ and a Mettler Toledo DSC 1 instrument were used for the DSC measurements to evaluate the thermal responses of the samples. The measurements were performed by two consecutive scans of cooling and subsequent heating of the samples in the temperature range of −80 °C to 150 °C for all systems except PTMC-C ($M_n = 220$) where −100 °C was used. The cooling rate was set to 5 K min^{-1} and the heating rate to 10 K min^{-1}.

Electrochemical impedance spectroscopy (EIS)

The total ionic conductivity of the SPE was measured by EIS in the temperature range of 25−80 °C. An SP-240 Potentiostat and a VMP3 Potentiostat from Bio-Logic were used to determine the impedance response. The measurements were performed in the 1 MHz to 1 Hz frequency range with an applied AC amplitude of 10 mV. The samples were measured in a Swagelok cell with two identical stainless-steel blocking electrodes with a diameter of 4 mm and a set thickness of 100 μm, employed by utilizing a polytetrafluoroethylene spacer (Figure S1). A typical Nyquist plot from EIS measurements can be seen in Figure S2.

Rheology

The melt viscosities of the SPEs were measured using a DHR20 Rheometer from TA Instruments. Most measurements were made using the environmental test chamber (ETC) accessory under constant nitrogen gas flow. For low-viscosity samples, the Peltier plate accessory was used. The SPEs were prepared inside an Argon-filled atmosphere and loaded to the rheometer immediately after being exposed to air. The geometry of the system was two parallel plates, either 25, 40 or 60 mm in diameter, depending on the viscosity of the sample. The gap was set between 0.5–1 mm. The geometry used for each sample can be seen in Table S1. Measurements were made at different temperatures, ranging from 30–100 °C. At each temperature, the system was allowed to equilibrate for 120 seconds. A frequency sweep was then run at a constant strain rate of 1 %. The complex dynamic viscosity was extracted from the plateau region of the sweep. The Cox–Merz transformation was then used to obtain the steady-flow viscosity from the complex dynamic viscosity.[15] A representative curve of a frequency sweep can be seen in Figure S3. For PEO-C and PTMC-C samples with $M_n = 220$ g mol^{-1}, the viscosity was determined with a DMA 4100 M density meter from Anton Paar in the temperature range of 30–80 °C.

Transference number measurements

The lithium transference numbers for the SPEs were determined by the Bruce–Vincent method with an SP-240 Potentiostat from Bio-Logic.[16] Symmetrical Li||Li cells for the measurements were prepared in pouch cells. The SPEs for these measurements were prepared by solution casting in the same manner as previously mentioned but with an additional glass fiber separator in the molds. The separator was added solely to contribute to the physical separation between the lithium electrodes, as the M_n of the SPEs was too low to provide self-standing films. The measurements were performed at either 25 °C or at 60 °C, based on the reactivity of the SPEs and the impedance response observed at 60 °C. Since the T_+ is marginally affected by the temperature unless very high salt concentrations are used, the obtained values are considered comparable.[17] The cells were allowed to equilibrate until the impedance response was stable prior to the measurement at the set temperature. The EIS measurement was performed in the frequency range of 7 MHz to 100 mHz with an AC amplitude of 10 mV, where a potential bias of 0 mV was applied before polarization and 10 mV after polarization, respectively. In between the EIS measurements, the cells were polarized by applying a 10 mV potential to the cells until a steady-state current was obtained. The initial current was calculated by utilizing Ohm's law from the total resistance in the cell and applied voltage, which is applicable in the absence of a concentration gradient.[18]

Fourier Transform Infrared Spectroscopy (FTIR)

ATR-FTIR measurements for ion coordination strength determination were performed with a VERTEX 70v FT-IR Spectrometer from Bruker with an RT-DLaTGS detector and a Quest ATR Accessory with a Diamond heated puck from Specac. The spectra were recorded with 15 °C temperature intervals from 25 °C up to 85 °C with 32 scans and a resolution of 4 cm^{-1}.

Density measurements

The density of the investigated samples where determined with a 5 ml glass pycnometer. For the measurements about 0.1–0.5 g of the samples was used with cyclohexane as a working liquid. For the lowest-M_n samples, the density was determined with a DMA 4100 M density meter from Anton Paar.

Results and Discussion

The physical and ion transport properties of PTMC and PEO with OH end groups or end-capped according to Figure 1 were investigated in the M_n range from 220 g mol^{-1} up to 4000 g mol^{-1}, *i.e.* the range where it has been shown previously that the ion transport properties change rapidly.[5b,c] In Table 1, the investigated samples in this study are shown. PTMC and PEO will be used to denote all samples with these polymer

Table 1. The M_n of the investigated samples, all with a salt concentration of $r = [LiTFSI]/[O] = 0.1$. Samples ending with OH have hydroxyl groups on the end of the chains, while the end-capped samples ending with C have the end group structures seen in Figure 1.

Sample	M_n / g mol^{-1}	Sample	M_n / g mol^{-1}
PTMC-OH	400	PEO-OH	300
	600		600
	850		1000
	1070		2000
	2000		4000
	4250		
PTMC-C	220	PEO-C	220
	320		500
	530		1000
	1040		2000
	2060		

structures, while PTMC-OH, PTMC-C, PEO-OH and PEO-C will be used to denote the specific end-group chemistry. Throughout the study, the salt concentration for all investigated systems is set to $r = [\text{LiTFSI}]/[\text{O}] = 0.1$ (O indicates the coordinating group in the polymer structure).

Glass transition temperature

The glass transition temperature (T_g) dependence on the M_n of the investigated SPEs is shown in Figure 2, where the data is fitted to the relationship described by Fox and Flory (the linear regression is shown in Figure S4):

$$T_g = T_{g,\infty} - \frac{K}{M_n} \quad (1)$$

where $T_{g,\infty}$ is the glass transition temperature at infinite chain length and K is a parameter related to the free volume in the system.[19] Due to the relatively high salt concentration ($r = 0.1$) and low molecular weight, all samples remained amorphous throughout the full temperature range, despite pure PEO being partially crystalline at room temperature above 1000 g mol^{-1}. As observed in Figure 2, low T_g values are obtained for the low-M_n samples, an effect originating from the larger concentration of end groups – regardless of their chemical identity – which have greater mobility than repeating units within the polymer chains leading to more free volume and a lower T_g. Considering the influence of the chemistry of the end groups at low M_n, a lower T_g is obtained for PEO with the non-polar CH_3 end groups than the samples with polar OH end groups, while a slightly lower T_g is observed for PTMC-C than PTMC-OH (Figure S4). This is an interaction effect, arising from the OH end groups forming stronger intermolecular interactions with the surrounding molecules and ions, which slows down the local dynamics, leading to a decreased free volume in the samples and ultimately a higher T_g.[20] At higher M_n, the T_g approaches a maximum temperature plateau ($T_{g,\infty}$), as the concentration of end groups in the system becomes negligible, following Eq. 1.[19] This is indeed observed for both polymers. The T_g for PEO samples is, as expected, lower than for PTMC samples as a consequence of the more flexible chains. The T_g for PEO with the lowest M_n could not be confirmed experimentally since the T_g was outside the temperature limits for the instrument (Figure S5). In a previous study, it was shown by Hayamizu et al. that PEO-C 220 (tetraglyme) with LiTFSI at the same concentration ($r = 0.1$) has a T_g of −80 °C.[10]

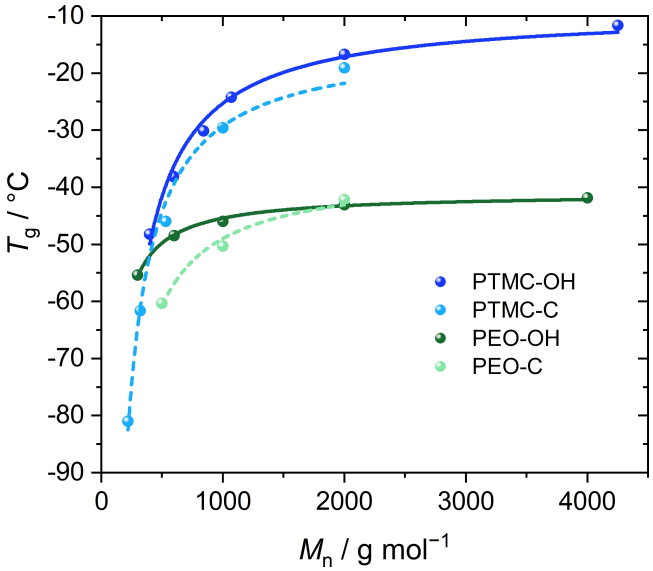

Figure 2. Determined T_g as a function of M_n for LiTFSI in PTMC-OH, PTMC-C, PEO-OH and PEO-C. The data have been fitted with the Flory–Fox equation.

Viscosity

To understand how the macroscopic mobility of the samples is affected by the polymer chain length, the viscosity (η) was determined for a range of temperatures. By using the Cox–Merz transformation, the steady-state viscosity could be determined from frequency sweeps at each temperature. The viscosity was measured both with and without LiTFSI, to attain information about the impact of the salt. Furthermore, to avoid crystallinity effects in the PEO samples without LiTFSI, the measurements were run above the melting point of the samples.

To analyze the effect of M_n, the viscosities at 60 °C were plotted against M_n. In Figure 3a, the PEO-OH and PTMC-OH series are plotted with and without LiTFSI. When plotted in a logarithmic scale, linear relationships are observed. These series are then fit against the de Gennes theory for polymer melts:

$$\eta \propto M_n^{\,b} \quad (2)$$

According to the Rouse model, the viscosity is proportional to M_n for short linear unentangled chains giving that $b = 1$.[21]

This relationship holds up to a critical molecular weight (M_c) above which chain entanglements exist and the viscosity is proportional to M_n to the power of 3.4, as described by de Gennes.[22] The PEO-OH series is well in line with previous literature,[5b,9] showing an excellent fit ($R^2 > 0.99$) and a slope close to unity in the measured range. Doping with LiTFSI leads to an upward shift in the viscosity, which is expected due to the strong coordination of PEO to Li^+, which acts as physical crosslinks. The slope remains the same ($b = 1$). This aligns well with previous studies on short-chain PEO, which follows the Rouse model up until around 6000 g mol^{-1}.[5b]

Unlike PEO-OH, the viscosity of PTMC-OH increases steeply in the whole investigated M_n interval. In fact, the viscosity increases with M_n to the power of 3.2, which is similar to the value predicted for entangled linear polymers above M_c. This is valid for both the series doped with LiTFSI and the pure PTMC-OH series. Indeed, the M_c has previously been determined to be 1000 g mol^{-1} for pure PTMC-OH.[23] These results suggest that it may be even lower, and underlines the significant difference in rheological properties between PTMC-OH and PEO-OH. When comparing these two polymer systems, it is worth keeping in mind that the PEO-OH series appears to be in the unentangled

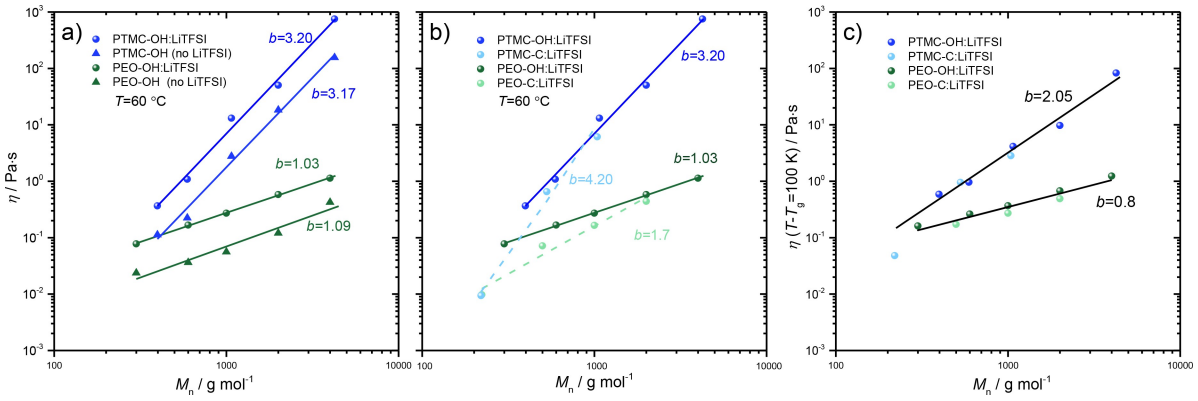

Figure 3. Steady-state viscosity (η) as a function of M_n (a) for PTMC-OH and PEO-OH with and without LiTFSI at 60 °C and (b) PTMC-OH, PTMCC, PEO-OH and PEOC with LiTFSI at 60 °C and (c) at reduced temperature. The reduced temperature $T-T_g = 100$ K was chosen to ensure the extracted temperatures were within the measurement range. Linear fits are made according to the de Gennes theory (Eq. 2) to determine the slope *b*.

regime, where the Rouse model holds, while the response for the PTMC-OH system suggests it is in the entangled regime, which leads it to deviate from the Rouse model.

In Figure 3b, the effect of the end group on the viscosity is shown. The less polar end-capped groups lead to a lower viscosity for PTMC-C and PEO-C compared to the OH series, which also correlates well with the lower T_g. This response originates from the increasing influence of the end group at lower M_n, where the OH end groups, as mentioned above, form intermolecular interactions to a greater extent, rendering a larger slope for PTMC-C and PEO-C compared to PTMC-OH and PEO-OH, respectively. However, by plotting the viscosity at a given constant friction factor ($T-T_g$), the effect from chain mobility can be removed. This was shown by Devaux et al.[5b] for PEO-OH and capped PEO, where the series collapsed onto the same line (at $b = 1.1$). By plotting the reduced viscosity of PTMC and PEO in Figure 3c, the same outcome is indeed obtained where the viscosity of the OH and end-capped series collapse into the same line ($b = 2.05$ for PTMC and $b = 0.8$ for PEO). This indicates that the end groups have a minor influence on the η, and rather affect the free volume and the T_g of the samples, which in turn influences the viscosity. Considering the slopes in the reduced viscosity plots, the value for PEO can still be considered to be close to 1, in agreement with the de Gennes model. The slope for PTMC, on the contrary, indicates that it indeed contains chain entanglements which leads to a deviation from the Rouse model. Although the behavior differs for PTMC and PEO, all sample series could be fitted with the VFT equation, indicating that the mobility of the systems follows a temperature dependence typical for polymers above their T_g (Figures S6 & S7). In summary, the results indicate that the doping with LiTFSI leads to a clear increase in viscosity for both systems, suggesting that ion-induced physical crosslinks exist in both systems. The end groups have a minor effect on the viscosity, mainly coupled to the local chain mobility (T_g). In contrast, when removing the effect from chain mobility (in Figure 3c) the viscosity still displays a clear dependence on M_n and the chemical nature of the repeating units, related to the low M_c of PTMC, generating chain entanglements within the measured range.

Transference number (T_+) and ion coordination strength

The dependence of T_+ on M_n was determined for the systems through the Bruce–Vincent method and the results are shown in Figure 4a.[13] A short description of the method and why it was chosen to determine the T_+ is presented in the Supporting Information. At the highest M_n, the T_+ for both PEO series are approaching 0.1 while both PTMC-series are close to 0.8. These values are similar to previously determined T_+ for these systems, indicating that reasonable values are determined for reference and comparison.[3a,24] For PTMC-OH, the T_+ decreases to below 0.5–0.6 at low M_n, simultaneously as the electrolytes become less viscous and more liquid-like.

This is also close to T_+ values frequently observed for common organic liquid electrolytes (0.2–0.5).[25] When the chains become sufficiently short and their mobility sufficiently high, it has been assumed the ion transport mechanism can approach an ion–polymer co-diffusion mechanism, which is similar to the transport in typical liquid electrolytes.[26] As for PTMC-C, on the contrary, T_+ remains around 0.8 down to 1000 g mol^{-1}, before a slight decrease to 0.75 is observed at $M_n = 500$ g mol^{-1}.

For PEO-OH, as mentioned, T_+ approaches 0.1 at high M_n, consistent with previously measured T_+ for high-molecular-weight PEO.[3a,14] At lower M_n, T_+ increases, approaching 0.2 for the lowest measurable M_n sample and closing in on values determined for common liquid electrolyte systems. For PEO-C, the T_+ is increasing from 0.1 up to 0.4 when going from 500 to 220 g mol^{-1}. Precisely as for PTMC-C, the onset of the T_+ change is shifted to lower M_n before it approaches values in the range of common liquid electrolytes (compared to PTMC-OH where T_+ starts to decrease at higher M_n). For both OH systems, the T_+ was undeterminable for the lowest-M_n systems due to their reactivity with Li metal, making the interface resistances unstable and any attempt to derive T_+ unreliable.

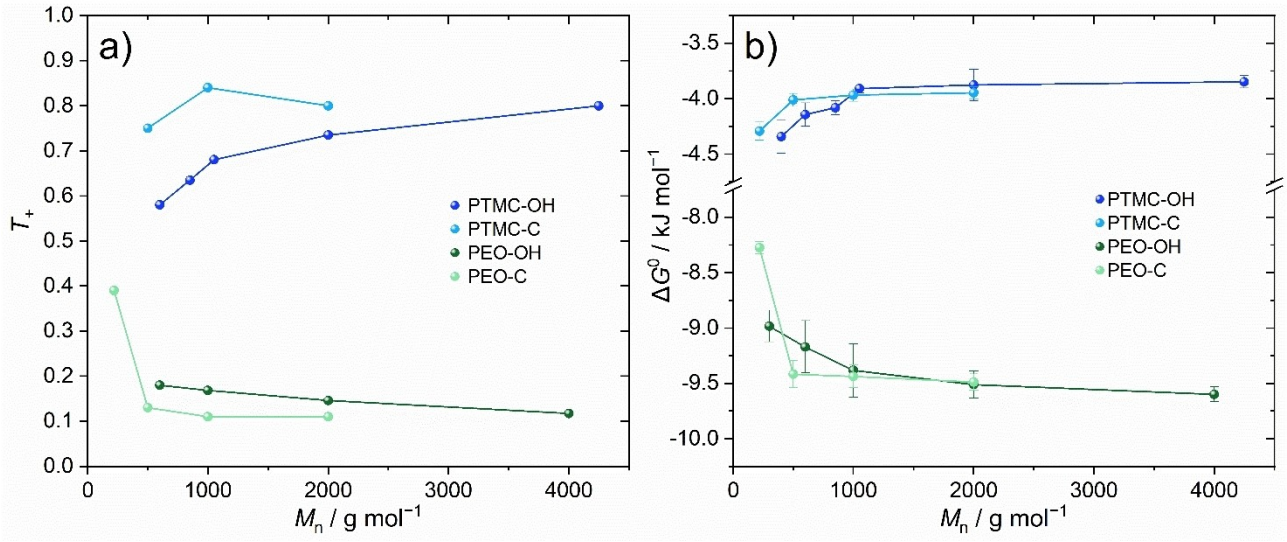

Figure 4. (a) Transference numbers determined with the Bruce–Vincent method and (b) calculated dissociation energy (ΔG^0) for LiTFSI in PTMC-OH, PTMC-C, PEO-OH and PEO-C and its dependence on Mn at 60 °C. Lines serve as a guide for the eye.[13a,b]

Interestingly, the trend seen in T_+ behavior correlates very well with the trend in ion coordination strength with molecular weight. FTIR measurements were employed to determine the ion coordination strength by deriving the LiTFSI dissociation energy (ΔG^0) in the systems, which in a solvent-free system can be used as an indirect measure of the coordination strength. In previous studies, it has been shown that a high coordination strength renders more dissociated salt and a low negative ΔG^0, which correlates with a high T_+ and *vice versa*.[3a,27] A brief explanation of the method is described in the Supporting Information. The quantitative nature of the method makes it advantageous to other methods that compare coordination environment in SPEs, such as using NMR.[27] In Figure 4b, ΔG^0 for LiTFSI in the investigated systems is shown. In general, there is only a small difference between the ΔG^0 of the OH and end-capped samples, except at the lowest M_n for the PEO series. The trends for both types of end groups are the same for each polymer, although it is noted that ΔG^0 for PEO-C and PTMC-C remains relatively unchanged until below $M_n = 500\ g\,mol^{-1}$, while it starts to increase for PEO-OH and decreases for PTMC-OH already below $M_n = 1000\ g\,mol^{-1}$.

The correlation with the T_+ trends for the systems is quite striking, even including the slight differences in behavior for the different end groups. The small differences between the end groups suggest that interactions of the OH end groups with the Li^+ cations only to a small extent cause the differences in coordination strength, while the main difference is caused by changes in the coordination structure that are dependent on the molecular weight. The difference in interaction strength between the OH and end-capped series seems to only account for the slight shift in M_n dependence between the series.

The perhaps most striking observation is the fact that the effect of the OH end groups for PEO-OH is completely reversed, further strengthening the conclusion that it is not the interaction of the group itself that is the main contributor to the observed effects. In a previous study, calculations showed that OH end groups have a higher binding energy to Li^+ than alkyl end groups. Despite this, a weaker coordination is seen for PEO-OH at low M_n. The calculations also showed that the OH end groups interacted more with $TFSI^-$ which also affects ΔG^0.[14] It seems like when the chains become shorter in PEO – regardless of end group – the chelation effect of the chains coordinating to Li^+ is gradually disrupted, thereby weakening the coordination and shifting the equilibrium towards TFSI anions coordinating with Li^+.[28] For PTMC, on the contrary, shorter chains increase the coordination strength, possibly as an effect of less optimal coordination between the carbonate oxygens in PTMC to Li^+ (compared for PEO), and where shorter chains are less sterically hindered to attain more optimally coordinating conformations. These observations also suggest that a gradual and continuous change in coordination environment occurs as a function of M_n, rather than distinct changes in ion transport mechanism.

Considering the general trends for T_+ and ΔG^0 and their dependence on the M_n, the previously observed correlation is again seen as the trends match each other. Correspondingly, strong coordination between the cation and the polymer backbone yields low T_+ and *vice versa*. These results reveal that the T_+ is highly dependent on the ion coordination strength, *i.e.* how strongly the ions are coordinated to the polymer in the system. Furthermore, the results illustrate that OH end groups have a small influence on the coordination strength and T_+, when the OH concentration is sufficiently high relative to the functional, coordinating group in the polymer backbone at low M_n (*e.g.* the ether oxygens in PEO and the carbonate oxygens in PTMC). Instead, the coordination structure seems to be dominant factor affecting the coordination strength.

Ionic conductivity

Although the change in T_+ with molecular weight has previously been attributed to a change in transport mechanism towards a "vehicular" co-diffusion at low M_n, the additional insight into the coordination strength suggests that this can explain a lot of the observed effects. Combining the T_+ data with the total ionic conductivity (σ_{tot}) of the PTMC and PEO electrolytes, we can determine the actual contributions of cations and anions to the ion transport in the systems to more closely examine any changes in the transport mechanism. In Figure 5, σ_{tot} is plotted as a function of M_n at 60 °C, showing a higher σ_{tot} for the PEO series compared to the PTMC series. A strong dependence on M_n is seen, where σ_{tot} decreases as M_n increases for all systems, and we furthermore see a significantly higher σ_{tot} at low M_n for the non-polar end-capped group series compared to the polar OH series. At M_n up to 2000 g mol^{-1}, the end group effect is still pronounced for both PTMC-C and PEO-C, but at sufficiently high M_n, it has previously been shown that PEO-C reaches the same σ_{tot} plateau value as PEO-OH.[5] This is expected for both systems at high M_n, since the concentration of end groups becomes negligible.

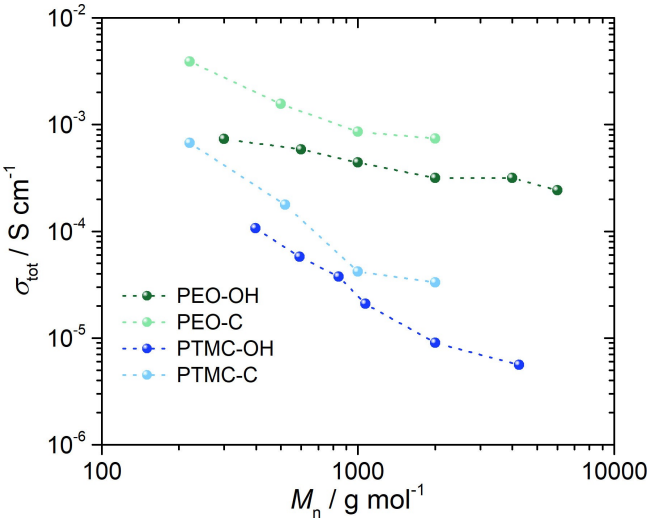

Figure 5. Total ionic conductivity (σ_{tot}) at 60 °C as a function of M_n for PTMC-OH, PTMC-C, PEO-OH and PEO-C with a salt concentration of $r = 0.1$.

By comparing the ionic conductivity dependence on the reduced temperature ($T - T_g + 50$ K) for the systems, the effect of different T_g is accounted for. This approach should minimize the effect of segmental motion and instead emphasize the structural and mechanistic effects on the ionic conductivity in the different systems. As seen in Figure 6a, approximately linear plots are observed, in agreement with the VFT equation. In addition, the effect of M_n almost completely disappears and each polymer system aggregates and basically falls onto a single line (Figure 6a). This indicates that σ_{tot} is solely governed by segmental motion, and not by different mechanisms that fall into discrete M_n ranges. A higher total ionic conductivity is also seen for all PEO systems compared to PTMC. The same trends are also observed when adjusting for the molar concentrations for all samples (Figure S10).

The differences in T_+ observed for the two polymer systems imply that Li^+ transport should be more facile in the weakly coordinating PTMC matrix. To investigate this further, σ_{Li} and σ_{TFSI} at reduced temperatures are plotted in Figures 6b and **c**, respectively. Strikingly, σ_{Li} for all systems are within the same order of magnitude (Figure 6b). In contrast, Figure 6c shows that σ_{TFSI} differs greatly between PEO and PTMC, where a significantly lower σ_{TFSI} is observed in PTMC. Thus, the differences in T_+ are not caused by differences in Li^+ mobility, but by differences in TFSI mobility, in line with previous observations for PEO and PCL.[3a] This indicates that the previous

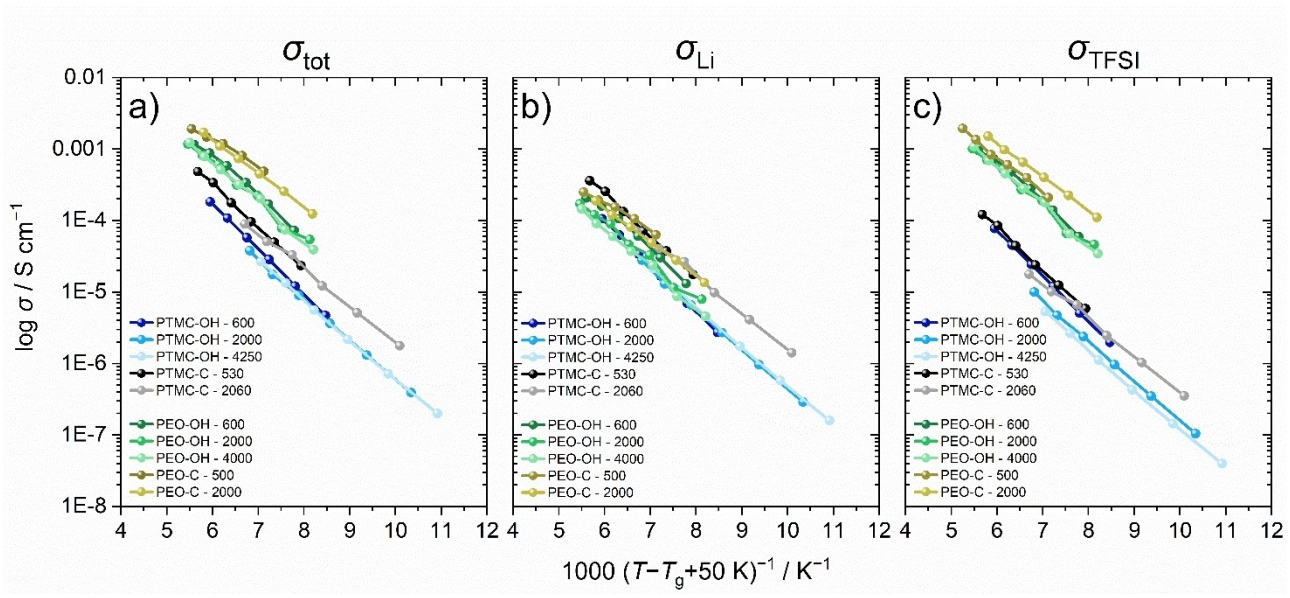

Figure 6. (a) The total ionic conductivity (σ_{tot}), (b) lithium-ion conductivity (σ_{Li}) and (c) TFSI anion conductivity (σ_{TFSI}) plotted versus 1000 $(T - T_g + 50\ K)^{-1}$. Partial ionic conductivities were calculated from the transference numbers obtained from the Bruce–Vincent method.

assumption of weaker coordination leading to higher Li^+ mobility may not be correct and that the underlying reason for the coupling of T_+ to the coordination strength is different, possibly involving cation–anion association (which is directly coupled to the coordination strength). Exactly what this mechanism entails remains to be determined.

Considering the impact of the end groups on the conductivities, Figure 6a shows that the samples with different end groups fall into two distinct groups, with an increased σ_{tot} for the end-capped systems. This suggests that there is an end group effect on the ion transport mechanism at low M_n. This effect seems to originate mainly from a higher σ_{Li} for the end-capped series at lower M_n and in combination with a higher σ_{TFSI} at high M_n. See Figure S11 for a clearer view. No clear trends can, however, be deciphered when comparing the two polymer systems more than that it seems like the OH groups interrupt the ion conduction by interacting with the ions, exhibiting a higher binding energy than alkyl groups. This was previously shown to be the case when the impact of different backbones was studied.[29] At higher M_n, however, the effect of the end groups on the ionic conductivities is anticipated to vanish, which has been shown previously to be the case for the PEO series.[5b]

The VFT behavior for the partial conductivities plots in Figure 6 suggests that the ion conduction is coupled to the chain relaxation similarly for all molecular weights regardless of the choice of end group. These results indicate that contrary to earlier assumptions, at least down to M_n ~500 g mol^{-1} of the investigated systems, the ion transport is mainly governed by the local chain dynamics. To the extent that chain entanglements in PTMC affect σ_{Li}, it would be by changing the local chain relaxation. The significant effect seen for the large-scale motion (viscosity) even at reduced temperature (Figure 3c) is, however, not reflected in σ_{Li}. Whether the chain entanglements have some effect on σ_{TFSI} remains uncertain at this point.

Conclusions

In this study, a comprehensive analysis of the effect of M_n on electrolytes based on the strongly ion-coordinating PEO and weakly coordinating PTMC was performed. Furthermore, the influence of OH and end-capped end groups in both systems was investigated. A significant difference was seen when comparing the viscosity of the two polymers, while PTMC displayed a higher viscosity, within the entanglement regime already at low M_n (below 2000 g mol^{-1}); the response for PEO remained in the unentangled regime for all measured M_n.

The M_n was also shown to have significant but opposite effects on the transference number of PEO and PTMC. At high M_n, a typical T_+ of 0.1 was seen for the PEO series, increasing at low M_n, with a significant increase at the lowest M_n for PEO-C. Conversely, the PTMC series displayed a typically high T_+ of 0.8 at high M_n, which decreased at lower M_n instead. The T_+ also correlated well with the coordination strength between Li and the polymer.

When accounting for T_g, the effect of M_n is eliminated and the partial conductivities suggest that the Li^+ conduction remains bound to the segmental motion even at the lowest M_n. No difference is seen between PTMC and PEO, despite PEO being in an unentangled regime while PTMC contains chain entanglements. Furthermore, the reduced temperature plot of the conductivity revealed that the difference in total ionic conductivity originates from the significantly lower *TFSI conductivity* in PTMC, while the Li conductivity is similar in both PEO and PTMC. Notably, the coordination strength does not seem to affect the Li mobility, which remains similar regardless of whether Li^+ is strongly or weakly coordinated to the polymer chains. Although these results corroborate the coupling of T_+ to coordination strength, the underlying cause of this needs to be reconsidered.

Supporting Information

The authors have cited additional references within the Supporting Information.[30]

Acknowledgements

The authors acknowledge financial support from the ERC (grant no. 771777 FUN POLYSTORE), The Swedish Research Council (grant number 2023-05456), Batteries Sweden (BASE), and STandUP for Energy.

Conflict of Interests

The authors declare no conflict of interest.

Data Availability Statement

The data that support the findings of this study are available from the corresponding author upon reasonable request.

Keywords: Lithium · polymers · molecular weight · ionic conductivity · transference number

[1] a) X. Q. Xu, X. B. Cheng, F. N. Jiang, S. J. Yang, D. Ren, P. Shi, H. Hsu, H. Yuan, J. Q. Huang, M. Ouyang, Q. Zhang, *SusMat* **2022**, *2*, 435–444; b) S. Wang, K. Rafiz, J. Liu, Y. Jin, J. Y. S. Lin, *Sustainable Energy and Fuels* **2020**, *4*, 2342–2351; c) F. Wu, Y.-X. Yuan, X.-B. Cheng, Y. Bai, Y. Li, C. Wu, Q. Zhang, *Energy Storage Mater.* **2018**, *15*, 148–170; d) C. Fang, J. Li, M. Zhang, Y. Zhang, F. Yang, J. Z. Lee, M.-H. Lee, J. Alvarado, M. A. Schroeder, Y. Yang, B. Lu, N. Williams, M. Ceja, L. Yang, M. Cai, J. Gu, K. Xu, X. Wang, Y. S. Meng, *Nature* **2019**, *572*, 511–515.
[2] M. Doyle, T. F. Fuller, J. Newman, *Electrochim. Acta* **1994**, *39*, 2073–2081.
[3] a) M. P. Rosenwinkel, R. Andersson, J. Mindemark, M. Schönhoff, *J. Phys. Chem. C* **2020**, *124*, 23588–23596; b) F. M. Gray, J. Connor, *Polymer electrolytes*, Royal society of chemistry, **1997**.
[4] B. Sun, J. Mindemark, E. V. Morozov, L. T. Costa, M. Bergman, P. Johansson, Y. Fang, I. Furó, D. Brandell, *Phys. Chem. Chem. Phys.* **2016**, *18*, 9504–9513.

[5] a) A. A. Teran, M. H. Tang, S. A. Mullin, N. P. Balsara, *Solid State Ionics* **2011**, *203*, 18–21; b) D. Devaux, R. Bouchet, D. Glé, R. Denoyel, *Solid State Ionics* **2012**, *227*, 119–127; c) K. Timachova, H. Watanabe, N. P. Balsara, *Macromolecules* **2015**, *48*, 7882–7888.
[6] a) J. Castillo, A. Santiago, X. Judez, I. Garbayo, J. A. Coca Clemente, M. C. Morant-Miñana, A. Villaverde, J. A. González-Marcos, H. Zhang, M. Armand, C. Li, *Chem. Mater.* **2021**, *33*, 8812–8821; b) Y. H. Chen, P. Lennartz, K. L. Liu, Y. C. Hsieh, F. Scharf, R. Guerdelli, A. Buchheit, M. Grünebaum, F. Kempe, M. Winter, G. Brunklaus, *Adv. Funct. Mater.* **2023**, *33*.
[7] P. Lennartz, B. A. Paren, A. Herzog-Arbeitman, X. C. Chen, J. A. Johnson, M. Winter, Y. Shao-Horn, G. Brunklaus, *Joule* **2023**, *7*, 1471–1495.
[8] a) R. Bernhard, A. Latini, S. Panero, B. Scrosati, J. Hassoun, *J. Power Sources* **2013**, *226*, 329–333; b) B. Sun, J. Mindemark, K. Edström, D. Brandell, *Electrochem. Commun.* **2015**, *52*, 71–74; c) S. Emilsson, V. Vijayakumar, J. Mindemark, M. Johansson, *Electrochim. Acta* **2023**, *449*, 142176.
[9] J. Shi, C. A. Vincent, *Solid State Ionics* **1993**, *60*, 11–17.
[10] K. Hayamizu, E. Akiba, T. Bando, Y. Aihara, *J. Chem. Phys.* **2002**, *117*, 5929–5939.
[11] D. Diddens, A. Heuer, O. Borodin, *Macromolecules* **2010**, *43*, 2028–2036.
[12] K. Ito, N. Nishina, H. Ohno, *J. Mater. Chem.* **1997**, *7*, 1357–1362.
[13] H. Y. Jung, P. Mandal, G. Jo, O. Kim, M. Kim, K. Kwak, M. J. Park, *Macromolecules* **2017**, *50*, 3224–3233.
[14] H. Hua, X. Yang, P. Zhang, J. Zhao, *J. Phys. Chem. C* **2023**, *127*, 17324–17334.
[15] W. P. Cox, E. H. Merz, *J. Polym. Sci.* **1958**, *28*, 619–622.
[16] a) P. G. Bruce, C. A. Vincent, *J. Electroanal. Chem. Interfacial Electrochem.* **1987**, *225*, 1–17; b) J. Evans, C. A. Vincent, P. G. Bruce, *Polymer* **1987**, *28*, 2324–2328.
[17] a) W. Gorecki, M. Jeannin, E. Belorizky, C. Roux, M. Armand, *J. Phys. Condens. Matter* **1995**, *7*, 6823–6832; b) K. Pożyczka, M. Marzantowicz, J. R. Dygas, F. Krok, *Electrochim. Acta* **2017**, *227*, 127–135.
[18] M. M. Hiller, M. Joost, H. J. Gores, S. Passerini, H. D. Wiemhöfer, *Electrochim. Acta* **2013**, *114*, 21–29.
[19] T. G. Fox, P. J. Flory, *J. Appl. Phys.* **1950**, *21*, 581–591.
[20] H. Ericson, A. Brodin, B. Mattsson, L. M. Torell, H. Rinne, F. Sundholm, *Electrochim. Acta* **1998**, *43*, 1401–1405.
[21] P. E. Rouse Jr., *J. Chem. Phys.* **1953**, *21*, 1272–1280.
[22] P. G. de Gennes, *J. Chem. Phys.* **1971**, *55*, 572–579.
[23] L. Timbart, M. Y. Tse, S. C. Pang, O. Babasola, B. G. Amsden, *Macromol. Biosci.* **2009**, *9*, 786–794.
[24] a) D. M. Pesko, K. Timachova, R. Bhattacharya, M. C. Smith, I. Villaluenga, J. Newman, N. P. Balsara, *J. Electrochem. Soc.* **2017**, *164*, E3569–E3575; b) T. Eriksson, A. Mace, J. Mindemark, D. Brandell, *Phys. Chem. Chem. Phys.* **2021**, *23*, 25550–25557; c) B. Sun, J. Mindemark, K. Edström, D. Brandell, *Solid State Ionics* **2014**, *262*, 738–742.
[25] a) S. Zugmann, M. Fleischmann, M. Amereller, R. M. Gschwind, H. D. Wiemhöfer, H. J. Gores, *Electrochim. Acta* **2011**, *56*, 3926–3933; b) P. Zhou, X. Zhang, Y. Xiang, K. Liu, *Nano Res.* **2023**, *16*, 8055–8071.
[26] C. Y. Son, Z.-G. Wang, *J. Chem. Phys.* **2020**, *153*.
[27] R. Andersson, G. Hernández, J. Mindemark, *Phys. Chem. Chem. Phys.* **2022**, *24*, 16343–16352.
[28] G. Åvall, J. Mindemark, D. Brandell, P. Johansson, *Adv. Energy Mater.* **2018**, *8*, 1703036.
[29] a) M. Ebadi, T. Eriksson, P. Mandal, L. T. Costa, C. M. Araujo, J. Mindemark, D. Brandell, *Macromolecules* **2020**, *53*, 764–774; b) D. M. Pesko, Y. Jung, A. L. Hasan, M. A. Webb, G. W. Coates, T. F. Miller, N. P. Balsara, *Solid State Ionics* **2016**, *289*, 118–124; c) Q. Zheng, D. M. Pesko, B. M. Savoie, K. Timachova, A. L. Hasan, M. C. Smith, T. F. Miller, G. W. Coates, N. P. Balsara, *Macromolecules* **2018**, *51*, 2847–2858; d) D. M. Pesko, M. A. Webb, Y. Jung, Q. Zheng, T. F. Miller, III, G. W. Coates, N. P. Balsara, *Macromolecules* **2016**, *49*, 5244–5255.
[30] A. Bakker, *Polymer* **1995**, *36*, 4371–4378.

Manuscript received: June 13, 2024
Revised manuscript received: August 5, 2024
Version of record online: October 2, 2024